Suppression of elliptic flow in a minimally viscous quark-gluon plasma

Huichao Song[1] and Ulrich Heinz[1, 2, *]

[1]*Department of Physics, The Ohio State University, Columbus, OH 43210, USA*
[2]*CERN, Physics Department, Theory Division, CH-1211 Geneva 23, Switzerland*
(Dated: February 1, 2008)

We compute the time evolution of elliptic flow in non-central relativistic heavy-ion collisions, using a (2+1)-dimensional code with longitudinal boost-invariance to simulate viscous fluid dynamics in the causal Israel-Stewart formulation. We show that even "minimal" shear viscosity $\eta/s = \hbar/(4\pi)$ leads to a large reduction of elliptic flow compared to ideal fluid dynamics, raising questions about the interpretation of recent experimental data from the Relativistic Heavy Ion Collider.

The success of the hydrodynamic model in describing the bulk of hadron production in Au+Au collisions at the Relativistic Heavy Ion Collider (RHIC) [1] has led to a paradigmatic shift in our view of the quark-gluon plasma (QGP): Instead of behaving like a gas of weakly interacting quarks and gluons [2], as naively expected on the basis of asymptotic freedom in QCD, its collective properties rather reflect those of a "perfect liquid" with (almost) vanishing viscosity. However, due to quantum mechanical uncertainty no fluid can have exactly zero viscosity [3], and recent work [4] on strongly coupled gauge field theories, based on techniques exploiting the AdS/CFT correspondence, suggests an absolute lower limit for the ratio of shear viscosity η to entropy density s: $\eta/s \geq \hbar/4\pi$. This raises the interesting question how close to this limit the actual value of the shear viscosity of the QGP created at RHIC is.

Answering this question requires hydrodynamic simulations for relativistic *viscous* fluids in which the ratio η/s enters as a parameter. To study the anisotropic ("elliptic") collective flow in non-central heavy-ion collisions, from which limits on η/s can be extracted [5], requires a code that evolves the hydrodynamic fields at least in the two dimensions transverse to the heavy-ion beam. In this Letter we present our first results from such simulations [6]; a longer paper with a discussion of all technical details of our approach is in preparation [7].

Relativistic hydrodynamics of viscous fluids is technically demanding. The straightforward relativistic generalization of the non-relativistic Navier-Stokes equation yields unstable equations that can lead to acausal signal propagation. A causally consistent theoretical framework was developed 30 years ago by Israel and Stewart [8]. It involves the simultaneous solution of hydrodynamic equations for a generalized energy-momentum tensor containing viscous pressure contributions, $\pi^{\mu\nu}(x)$, together with kinetic evolution equations, characterized by a (short) microscopic collision time scale τ_π, for the dynamical approach of $\pi^{\mu\nu}$ towards its Navier-Stokes limit. Compared to ideal fluid dynamics, this leads effectively to more than a doubling of the number of coupled partial differential equations to be solved [9].

The last couple of years have seen extensive activity in implementing the Israel-Stewart equations (and slight variations thereof) [8, 9, 10, 11, 12] numerically, for systems with boost-invariant longitudinal expansion and transverse expansion in zero [10, 12], one [11, 13, 14, 15] and two dimensions [16, 17] (see also Ref. [18] for a numerical study of the relativistic Navier-Stokes equation in 2+1 dimensions). It is probably fair to say that the process of verification and validation of these numerical codes is still ongoing: While different initial conditions and evolution parameters used by the different groups of authors render a direct comparison of their results difficult, it seems unlikely that accounting for these differences will bring the various published numerical results in line with each other.

We here present results obtained with an independently developed (2+1)-dimensional causal viscous hydrodynamic code, VISH2+1 [6, 19], which has been extensively tested (for details see [7]): (i) in the limit of vanishing viscosity, it accurately reproduces results obtained with the (2+1)-d ideal fluid code AZHYDRO [20]; (ii) for homogeneous density distributions (i.e. in the absence of density gradients) and vanishing relaxation time it accurately reproduces the known analytic solution of the relativistic Navier-Stokes equation for boost-invariant longitudinal expansion [3]; (iii) for very short kinetic relaxation times our Israel-Stewart code accurately reproduces results from a (2+1)-d relativistic Navier-Stokes code, under restrictive conditions where the latter produces numerically stable solutions; and (iv) for simple analytically parametrized anisotropic velocity profiles the numerical code correctly computes the velocity shear tensor that drives the viscous hydrodynamic effects.

VISH2+1 solves the equations for local energy-momentum conservation, $d_m T^{mn} = 0$, with

$$T^{mn} = e u^m u^n - p \Delta^{mn} + \pi^{mn}, \quad \Delta^{mn} = g^{mn} - u^m u^n, \quad (1)$$

together with kinetic equations for the viscous shear pressure π^{mn} [21],

$$D\pi^{mn} = \frac{1}{\tau_\pi}(2\eta\sigma^{mn} - \pi^{mn}) - (u^m\pi^{nk} + u^n\pi^{mk})Du_k. \quad (2)$$

Here $D = u^m d_m$ is the time derivative in the local co-moving frame and $\sigma^{mn} = \nabla^{\langle m} u^{n\rangle} = \frac{1}{2}(\nabla^m u^n + \nabla^n u^m) - \frac{1}{3}\Delta^{mn}d_k u^k$ (with $\nabla^m = \Delta^{ml}d_l$) is the symmetric and traceless velocity shear tensor. We use a fixed Eulerian space-time grid in curvilinear coordinates $x^m = (\tau, x, y, \eta)$, with longitudinal proper time $\tau = \sqrt{t^2 - z^2}$ and space-time rapidity $\eta = \frac{1}{2}\ln\frac{t+z}{t-z}$, where z is the beam direction and (x,y) are the two transverse directions. d_m indicates the covariant derivative in direction x^m in this coordinate system. As in Refs. [14, 15, 16, 17, 18] we neglect bulk viscosity and heat conduction as presumably subdominant effects in a QGP with approximately vanishing net baryon density.

We implement longitudinal boost-invariance via the ansatz $u^m = (u^\tau, u^x, u^y, u^\eta) = \gamma_\perp(1, v_x, v_y, 0)$, with $\gamma_\perp = (1 - v_x^2 - v_y^2)^{-1/2}$, using η-independent initial conditions. The equations to be solved are 3 hydrodynamic equations for $T^{\tau\tau}$, $T^{\tau x}$ and $T^{\tau y}$, together with 4 kinetic equations for $\pi^{\eta\eta}$, $\pi^{\tau\tau}$, $\pi^{\tau x}$ and $\pi^{\tau y}$ [7, 22]. To check the numerics we also evolved additional, redundant components of π^{mn} and confirmed that the identities $u_m\pi^{mn} = 0 = \pi^m_m$ are preserved over time.

Due to the limited size of the transverse (x,y) grid in our current code, we here present results only for Cu+Cu collisions; simulations of the larger Au+Au system will soon be forthcoming. We use standard Glauber model initial conditions [1], assuming wounded-nucleon scaling of the initial transverse energy density $e(x, y, \tau_0; b)$ [23], with a Woods-Saxon radius $R_{\rm Cu} = 4.2\,{\rm fm}$, surface thickness $\xi = 0.596\,{\rm fm}$, and equilibrium density $\rho_0 = 0.17\,{\rm fm}^{-3}$. We scale this profile to a peak initial energy density in central $(b=0)$ collisions of $e_0 = 30\,{\rm GeV/fm}^3$. This is higher than expected for Cu+Cu collisions at RHIC but ensures that the system spends enough time in the QGP phase to explore the effects of shear viscosity on the evolution of anisotropic flow in this phase. We start the hydrodynamic evolution at $\tau_0 = 0.6\,{\rm fm}/c$ with vanishing transverse flow, both for the viscous evolution and ideal fluid dynamical comparison runs. For the equation of state (EoS) we use a slight variation of EOS Q from Ref. [23] (which implements a phase transition at $T_{\rm c} = 164\,{\rm MeV}$ between a free quark-gluon gas above $T_{\rm c}$ and a chemically equilibrated hadron resonance gas below $T_{\rm c}$) where the sharp corners at either end of the Maxwell contruction at $T_{\rm c}$ are rounded off for numerical stability [24]. Neither the initial conditions nor the EoS have been fine-tuned for a realistic comparison with experimental data; we here emphasize the comparison between ideal fluid and viscous hydrodynamic evolution, in order to identify qualitative differences between the two and to quantitatively understand their origin.

The viscous hydrodynamic equations contain two parameters, the shear viscosity η and the kinetic relaxation time τ_π. All simulations presented here are done with "minimal" viscosity [4] $\eta/s = 1/4\pi$, while τ_π is varied between $\frac{1}{2}$ (default) and $\frac{1}{4}$ of the classical Boltzmann gas
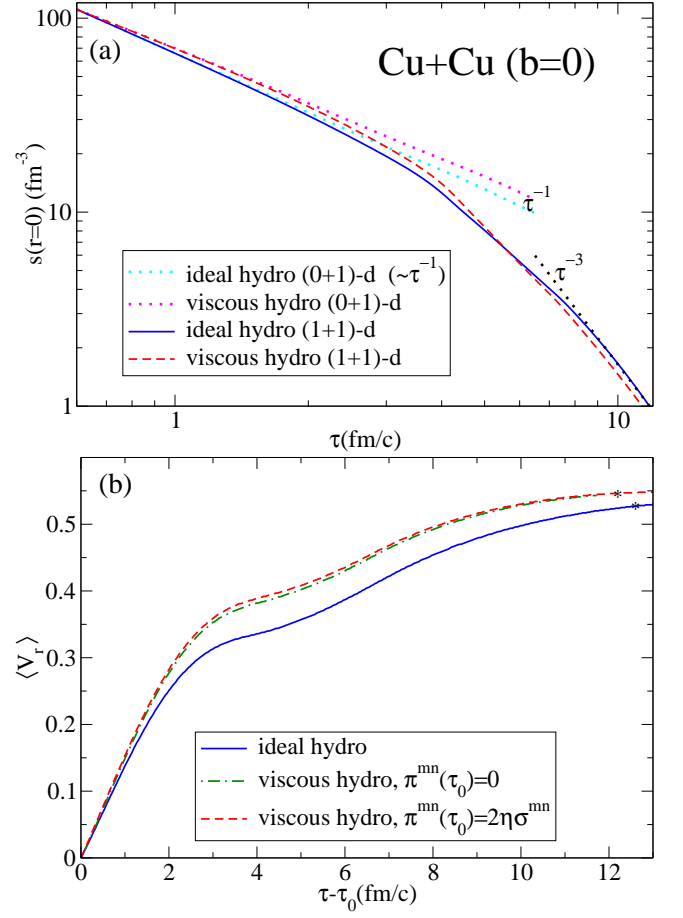

FIG. 1: (Color online) Time evolution of the central entropy density (a) and average radial flow velocity (b) in central Cu+Cu collisions (see text for details). Here and later stars indicate the time when all matter is frozen out.

estimate $\tau_\pi^{\rm Boltz} = \frac{6\eta}{4p} = \frac{6}{T}\frac{\eta}{s}$ [8, 25].

In Figure 1 we show the evolution of the central entropy density $s(r=0)$ and the average radial flow $\langle v_r\rangle$ (with the Lorentz contracted energy density $\gamma_\perp e$ as weight function) for central $(b=0)$ Cu+Cu collisions. The curves labeled "(0+1)-d" correspond to 1-dimensional boost-invariant longitudinal expansion without transverse flow (i.e. to transversally homogeneous initial conditions). One sees that in this case (which, for a simple EoS and in the Navier-Stokes limit, can be solved analytically [3]) shear viscosity reduces the cooling rate, due to a well-known *reduction of the work done by longitudinal pressure* [3] – additional entropy is produced, and the entropy density decreases more slowly than the $1/\tau$-law for ideal fluids. For transversally inhomogeneous initial conditions ("(1+1)-d hydro"), the developing radial flow increases the cooling rate compared to the case without transverse expansion, for both ideal and viscous fluid dynamics. However, in this case the shear viscous effects *increase the transverse pressure* relative to the ideal fluid case, leading to a faster build-up of radial flow (bottom

panel in Fig. 1), which in turn accelerates the cooling of the fireball center in such a way that by the time the expansion becomes effectively three-dimensional (indicated by the τ^{-3} line in Fig. 1(a)) the viscous fluid cools *more rapidly* than the ideal one [11]. (This was also seen (although not emphasized) in Refs. [11, 14, 15, 16].) The larger radial flow of the viscous fluid (Fig 1(b)) leads to flatter final transverse momentum spectra [14, 15, 16, 27], but (as pointed out in [15, 27]) this effect can be largely compensated by starting the viscous hydrodynamic evolution later and with lower initial energy density.
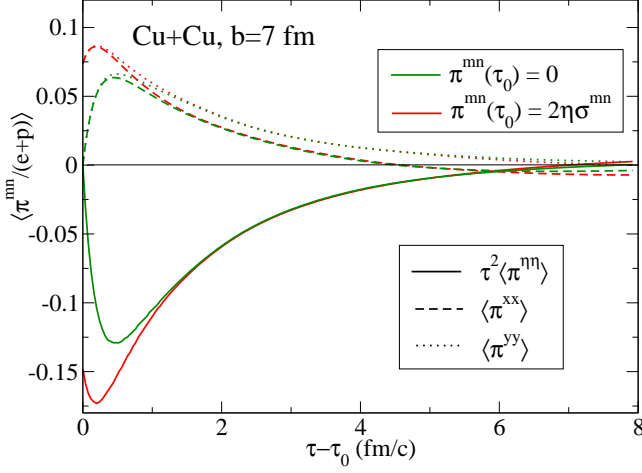

FIG. 2: (Color online) Time evolution of the dominant components of the shear viscous pressure tensor, normalized by $e+p$ and averaged over the transverse plane, for two different initial conditions (red and green, respectively). Note that the normalization factor $e+p \sim T^4$ decreases rapidly with time.

The dotted and dash-dotted lines in Fig. 1(b) show that (at least for the short relaxation time $\tau_\pi = \frac{1}{2}\tau_\pi^{\text{Boltz}} = 0.24\left(\frac{200\,\text{MeV}}{T}\right)$ fm/c considered here) the initial conditions for the shear viscous pressure tensor don't matter much: whether π^{mn} is initially taken to vanish or to assume its Navier-Stokes limit $2\eta\sigma^{mn}$, it quickly relaxes to the same function at times $\tau - \tau_0 \gtrsim 4\tau_\pi \approx 1$ fm/c. This is seen more explicitly in Fig 2 where we show, for non-central Cu+Cu collisions at $b = 7$ fm and the same two sets of initial conditions for the viscous shear pressure tensor, the time evolution of the dominant components of π^{mn}, normalized to the equilibrium enthalpy $e+p$ (which sets the scale for the energy-momentum tensor in the ideal fluid limit) and averaged over the transverse plane. Other components of $\langle\pi^{mn}\rangle$ are at least an order of magnitude smaller than the ones shown. The signs of $\langle\pi^{\eta\eta}\rangle < 0$ and $\langle\pi^{xx}\rangle, \langle\pi^{yy}\rangle > 0$ reflect the reduced longitudinal and increased transverse pressure caused by shear viscosity. The negative difference $\langle(\pi^{xx}-\pi^{yy})/(e+p)\rangle < 0$ seen in Fig. 2 causes a significant viscous reduction of the total momentum anisotropy ϵ_p which we discuss next.

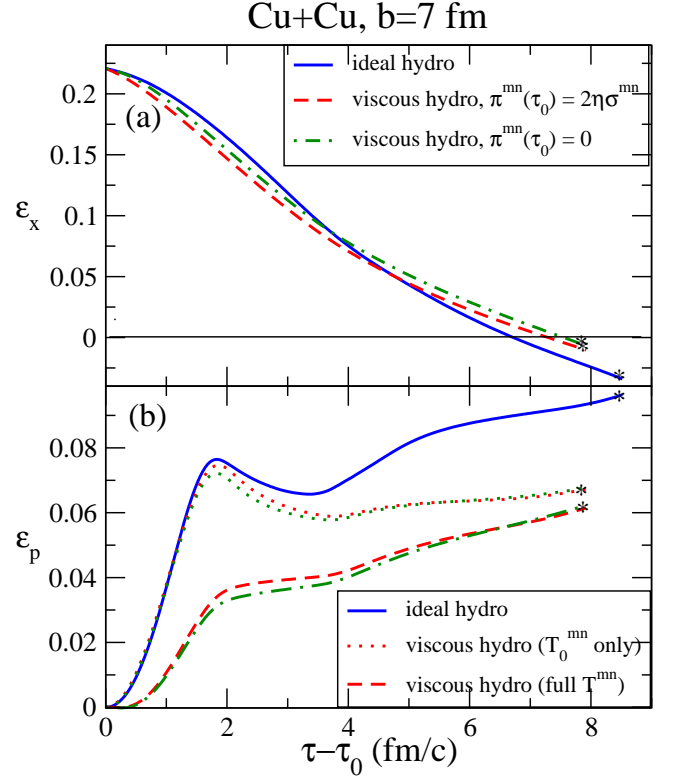The anisotropic flow is driven by the spatial source

FIG. 3: (Color online) Time evolution of the spatial eccentricity ϵ_x (a) and momentum anisotropy ϵ_p (b) for non-central Cu+Cu collisions at $b = 7$ fm. See text for details.

eccentricity $\epsilon_x = \frac{\langle y^2 - x^2 \rangle}{\langle y^2 + x^2 \rangle}$ (where $\langle\ldots\rangle$ denotes the energy density weighted average over the transverse plane [1]) and the anisotropic pressure gradients it generates. Fig. 3a shows that it decreases as a function of time, and does so more rapidly initially, but more slowly later for the viscous fluid than in ideal hydrodynamics. The initial drop rate for ϵ_x depends on the initial value for the viscous pressure tensor, but after about 1 fm/c different initializations for π^{mn} lead to parallel evolution histories for ϵ_x. The largest initial decrease for ϵ_x is observed for the largest initial viscous pressure tensor; initial free-streaming of the matter would correspond to an extreme case of viscous fluid dynamics, leading to even larger initial π^{mn} and even faster initial decrease of the spatial eccentricity than shown in Fig. 3a [28].

In Fig. 3b we plot, for ideal and viscous hydrodynamic evolution, the total momentum anisotropy averaged over the transverse plane, $\epsilon_p = \frac{\langle T^{xx} - T^{yy}\rangle}{\langle T^{xx} + T^{yy}\rangle} = \frac{\langle T_0^{xx} + \pi^{xx} - T_0^{yy} - \pi^{yy}\rangle}{\langle T_0^{xx} + \pi^{xx} + T_0^{yy} + \pi^{yy}\rangle}$, as a function of time. The closely spaced green and red lines distinguish different initializations for π^{mn}, as specified in Fig. 3a, showing weak sensitivity to these initial values. More interesting is the separation of the contributions to ϵ_p arising from the ideal fluid part T_0^{mn} (which only tracks the differences in the evolution of flow velocity and thermal pressure between

ideal and viscous hydrodynamics) and from the viscous pressure components π^{mn} (dashed and dotted lines in Fig. 3b). Initially, the viscous flow and thermal pressure evolution is not very different from the ideal fluid case, and it takes a while until the viscous pressure effects manifest themselves in a significant reduction of the flow anisotropy, thereby modifying the ideal fluid part T_0^{mn} of the energy momentum tensor. However, the viscous pressure components π^{mn} contribute themselves a negative, initially large part to the total momentum anisotropy, resulting (for $\frac{\eta}{s} = \frac{1}{4\pi}$) in an overall reduction of the latter by almost 50% relative to the ideal fluid case *over the entire time history*. At late times, the viscous pressure components become small, but by then their negative effect on the buildup of elliptic flow has fully manifested itself in the collective flow profile and is thus carried by the ideal fluid part T_0^{mn} of the energy momentum tensor.
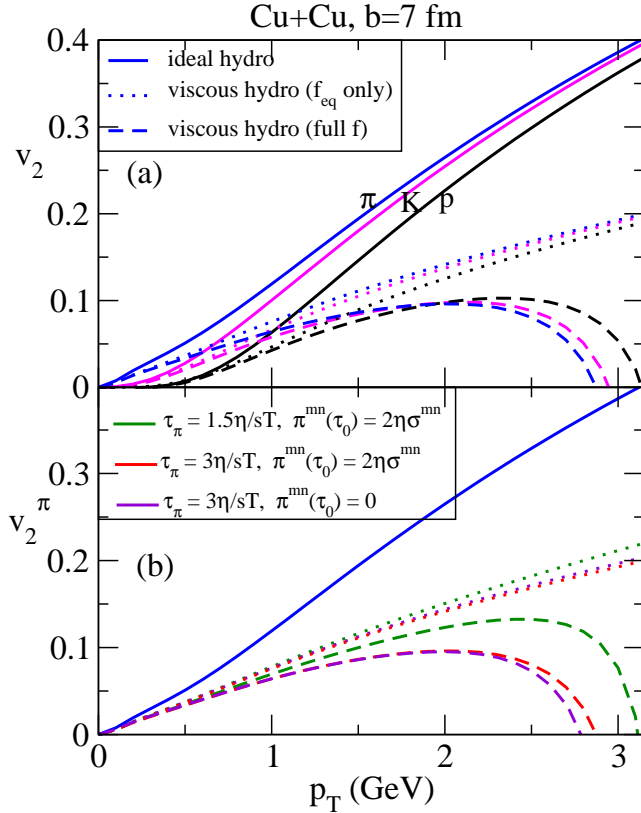

FIG. 4: (Color online) (a) The elliptic flow $v_2(p_T)$ for pions, kaons and protons from ideal fluid dynamics (solid lines) and viscous hydrodynamics (dotted and dashed lines). Dotted lines account only for viscous effects on the flow pattern that enters the equilibrium part of the distribution function; dashed lines additionally include viscous (non-equilibrium) corrections to the latter. (b) Effects of different choices for the kinetic relaxation time τ_π and for the initial viscous pressure π^{mn} on pion elliptic flow (with the same separation of equilibrium and non-equilibrium contributions as in part (a)).

The elliptic flow $v_2^{(i)} = \langle \cos(2\phi_p) \rangle_i$, calculated as the

$\cos(2\phi_p)$-moment of the observed hadron momentum distribution $\frac{dN_i}{dy\, p_T dp_T\, d\phi_p}$, depends on particle species i and measures the distribution of the total momentum anisotropy ϵ_p over the various hadron species and over transverse momentum p_T. This distribution depends on the chemical composition of the fireball at kinetic freeze-out, here assumed (unrealistically) to be a chemically equilibrated hadron resonance gas. The hadron momentum distributions are calculated as a Cooper-Frye integral [1] over a decoupling surface Σ of constant temperature $T_{\text{dec}} = 130\,\text{MeV}$:

$$\frac{dN_i}{dy p_T dp_T d\phi_p} = \int_\Sigma \frac{p \cdot d^3\sigma(x)}{(2\pi)^3} \left[f_{\text{eq}}^{(i)}(x,p) + \delta f^{(i)}(x,p) \right]$$
$$= \int_\Sigma \frac{p \cdot d^3\sigma(x)}{(2\pi)^3} \, f_{\text{eq}}^{(i)}(x,p) \qquad (3)$$
$$\times \left[1 + \left(1 - f_{\text{eq}}^{(i)}(x,p)\right) \frac{1}{2} \frac{p^m p^n}{T^2(x)} \frac{\pi_{mn}(x)}{(e+p)(x)} \right].$$

Here $f_{\text{eq}}^{(i)}\left(\frac{p \cdot u(x)}{T(x)}\right)$ is the local thermal equilibrium distribution function with temperature $T(x)$, boosted to the laboratory frame by the local hydrodynamic flow velocity $u^m(x)$ – both taken from the hydrodynamic output on the freeze-out surface Σ (whose normal vector is $d^3\sigma(x)$). $\delta f^{(i)}$ describes the deviation from local thermal equilibrium due to viscous effects and is given by the last term in the bottom line of Eq. (3) [5, 12]. It is proportional to the viscous pressure tensor π^{mn}, and even though (in contrast to early times) $\pi^{mn}(x)$ is small on the freeze-out surface, its effect on the distribution function grows quadratically with momentum, leading to a breakdown of the (viscous) hydrodynamic calculation of hadron spectra at sufficiently large p_T (in our case $|\delta N^\pi(p)/N_{\text{eq}}^\pi(p)| > 50\%$ for $p_T > 2.5\,\text{GeV}/c$ where $N^\pi(p)$ denotes the pion momentum spectrum).

In Fig. 4 we compare, for a few common hadron species, the elliptic flow $v_2(p_T)$ from ideal and viscous fluid dynamics. One sees that even "minimal" shear viscosity $\frac{\eta}{s} = \frac{1}{4\pi}$ causes a dramatic suppression of elliptic flow. The effects seen in Fig. 4 seem to be even larger than those reported in [17] – this discrepancy clearly calls for clarification [30]. Even without accounting for the slight deviations δf of the distribution function from its thermal equilibrium form, caused by small but non-vanishing shear pressure tensor components on the freeze-out surface, we see that elliptic flow is reduced by almost 50% (dotted lines in Fig. 4), due to the already mentioned reduction of azimuthal anisotropies of the hydrodynamic flow field. This effect was not even considered by Teaney in [5] when he attempted to constrain the shear viscosity of the QGP using RHIC v_2 data. Teaney's argument was entirely based on the viscous corrections $\delta f \sim p^m p^n \pi_{mn} \sim p_T^2$ arising from non-vanishing viscous pressure on the freeze-out surface (the difference between the dotted and dashed lines in Fig. 4) which, at

low p_T, is a much smaller effect. His phenomenological limit [5] on the shear viscosity of the fireball matter created at RHIC is therefore not restrictive enough: even a superficial comparison of the shapes of the $v_2(p_T)$ curves in Fig. 4 with experimental data [1] suggests that *RHIC data may be inconsistent with the conjectured lower limit $\frac{\eta}{s} = \frac{1}{4\pi}$ for the QGP shear viscosity.*

This conclusion, even though tentative since it is not yet based on a quantitative data comparison with calculations that use a more realistic EoS and better initial conditions, appears to be robust since neither a 100% variation of the initial value for π^{mn} nor a 50% reduction of the kinetic relaxation time for the viscous pressure tensor (see Fig. 4b) are able to significantly attenuate the strong viscous reduction of elliptic flow that we see in our calculations. While it supports the new paradigm of the "perfect fluidity" of the QGP created at RHIC, a possible violation of the conjectured "minimum viscosity bound" [4] is a serious matter that raises the question whether other explanations might be possible. Among the possibilities that one might contemplate are that the initial spatial source eccentricity in RHIC collisions has been significantly underestimated [29] or that a realistic equation of state is effectively stiffer than the one used here. T. Cohen and collaborators [31] have advanced counter examples of theories that appear to contradict the existence of a universal "minimum viscosity bound", although these examples to not include QCD. Our findings suggest that QCD might belong to the list of exceptions. Lublinsky and Shuryak [32] have shown that higher order corrections to the Israel-Stewart theory of viscous relativistic hydrodynamics tend to decrease viscous entropy production, so there may be a possibility that they also reduce viscous effects on the elliptic flow [30]. If this turns out to be case, our tentative conclusion as formulated above is premature. Obviously all these issues must be carefully investigated before a complete understanding of the RHIC data can be achieved.

---

* Correspond to heinz@mps.ohio-state.edu

[1] P. Huovinen, in *Quark Gluon Plasma 3*, edited by R. C. Hwa and X. N. Wang (World Scientific, Singapore, 2004), p. 600 [nucl-th/0305064]; P. F. Kolb and U. Heinz, *ibid.*, p. 634 [nucl-th/0305084].

[2] B. Müller, *The Physics of the Quark-Gluon Plasma*, Springer Lecture Notes in Physics, Vol. 225 (Springer-Verlag, Berlin, 1985).

[3] P. Danielewicz and M. Gyulassy, Phys. Rev. D **31**, 53 (1985).

[4] G. Policastro, D. T. Son and A. O. Starinets, Phys. Rev. Lett. **87**, 081601 (2001); and JHEP **0209**, 043 (2002); P. Kovtun, D. T. Son and A. O. Starinets, Phys. Rev. Lett. **94**, 111601 (2005).

[5] D. Teaney, Phys. Rev. C **68**, 034913 (2003).

[6] A preliminary account of this work, before all checks of our numerical code were completed, can be found at http://pirsa.org/07050047 (May 2007).

[7] H. Song and U. Heinz, in preparation.

[8] W. Israel, Ann. Phys. (N.Y.) **100** (1976) 310; W. Israel and J. M. Stewart, *ibid.* **118** (1979) 341.

[9] U. Heinz, H. Song and A. K. Chaudhuri, Phys. Rev. C **73**, 034904 (2006).

[10] A. Muronga, Phys. Rev. Lett. **88**, 062302 (2002) [Erratum: *ibid.* **89**, 159901 (2002)]; Phys. Rev. C **69**, 034903 (2004); *ibid.* **76**, 014909 and 014910 (2007).

[11] D. A. Teaney, J. Phys. G **30**, S1247 (2004).

[12] R. Baier, P. Romatschke and U. A. Wiedemann, Phys. Rev. C **73**, 064903 (2006).

[13] A. Muronga and D. H. Rischke, arXiv:nucl-th/0407114.

[14] A. K. Chaudhuri and U. Heinz, J. Phys. Conf. Ser. **50**, 251 (2006);

[15] R. Baier and P. Romatschke, Eur. Phys. J. C **51**, 677 (2007); P. Romatschke, *ibid.* **52**, 203 (2007).

[16] A. K. Chaudhuri, arXiv:0704.0134 [nucl-th]; and arXiv:0708.1252 [nucl-th].

[17] P. Romatschke and U. Romatschke, arXiv:0706.1522 [nucl-th].

[18] A. K. Chaudhuri, Phys. Rev. C **74**, 044904 (2006);

[19] The acronym stands for "**V**iscous **I**srael-**S**tewart **H**ydrodynamics in **2+1** space-time dimensions".

[20] AZHYDRO can be downloaded from URL http://nt3.phys.columbia.edu/people/molnard/OSCAR/.

[21] As pointed out in [12], the last term in Eq. 2 is needed to ensure that the time evolution of π^{mn} preserves its tracelessness and transversality to u^m. It was erroneously dropped in Ref. [9]. It vanishes identically for the (1+1)-d case discussed in [9] but not for (2+1)-d evolution.

[22] The explicit form of these equations is given in [9]. However, Eqs. (5.21b,c) and (5.29) in [9] must be corrected for contributions arising from the missing last term in Eq. (2) [12], and Eq. (5.21a) in [9] for a missing metric factor from the covariant derivative:
$\frac{1}{\tau^2}(\partial_\tau + v_x \partial_x + v_y \partial_y)(\tau^2 \pi^{\eta\eta}) = -\frac{1}{\gamma_\perp \tau_\pi}(\pi^{\eta\eta} - 2\eta\sigma^{\eta\eta})$.

[23] P. F. Kolb, J. Sollfrank and U. Heinz, Phys. Rev. C **62**, 054909 (2000).

[24] Specifically, we smooth the discontinuities of the squared speed of sound c_s^2 (which vanishes in the mixed phase) at both ends of the mixed phase with a Fermi function, with width parameters $\Delta e = 0.1 \, \mathrm{GeV/fm^3}$ at the upper (QGP) end of the mixed phase and $\Delta e = 0.02 \, \mathrm{GeV/fm^3}$ at its lower (HG) end.

[25] This classical value is a bit large for comfort during the early expansion stage since, for consistency of the hydrodynamic approach, we would like to maintain the inequality $\tau_\pi (\partial \cdot u) \approx \frac{\tau_\pi}{\tau} \ll 1$ which ensures that the microscopic scattering time scale is shorter than the macroscopic expansion time scale. A much shorter value, such as the AdS/CFT motivated number $\tau_\pi = \tau_\pi^{\mathrm{Boltz}}/30$ [26], however, seems to be too close to the Navier-Stokes limit, generating numerical instabilities in the VISH2+1 evolution.

[26] M. P. Heller and R. A. Janik, Phys. Rev. D **76**, 025027 (2007).

[27] U. Heinz and S. M. H. Wong, Phys. Rev. C **66**, 014907 (2002).

[28] T. Hirano and U. Heinz, unpublished notes (2004).

[29] T. Hirano, U. Heinz, D. Kharzeev, R. Lacey and Y. Nara, Phys. Lett. B **636**, 299 (2006).

[30] We have some first indications [7] that viscous effects are larger in the smaller Cu+Cu collision system studied here than in the Au+Au collisions studied in [17]. We also note that the authors of [17] do not solve exactly the same equations as we do, but keep an additional term that is formally of higher order in the gradient expansion around local equilibrium, but appears to be numerically important and to reduce the strong viscous quenching of elliptic flow seen by us (Paul Romatschke, private communication).

[31] T. D. Cohen, Phys. Rev. Lett. **99**, 021602 (2007); A. Cherman, T. D. Cohen and P. M. Hohler, arXiv:0708.4201 [hep-th].

[32] M. Lublinsky and E. Shuryak, Phys. Rev. C **76**, 021901 (2007).